A Two-Stage Matching Method for Multi-Component Shapes

Reza HASSANPOUR
Cankaya University, Ankara - Turkey
reza@cankaya.edu.tr

***Abstract*—In this paper a shape matching algorithm for multiple component objects has been proposed which aims at matching shapes by a two-stage method. The first stage extracts the similarity features of each component using a generic shape representation model. The first stage of our shape matching method normalizes the components for orientation and scaling, and neglects minor deformations. In the second stage, the extracted similarity features of the components are combined with their relative spatial characteristics for shape matching. Some important application areas for the proposed multi-component shape matching are medical image registration, content based medical image retrieval systems, and matching articulated objects which rely on the a-priori information of the model being searched. In these applications, salient features such as vertebrae or rib cage bones can be easily segmented and used. These features however, show differences from person to person on one hand and similarities at different cross-sectional images of the same examination on the other hand. The proposed method has been tested on articulated objects, and reliable registration of 3-dimensional abdominal computed tomography images.**

***Index Terms*—Shape Matching, Articulated Shape Matching, Medical Image Processing.**

I. INTRODUCTION

Human visual system is capable of recognizing many objects based on their shapes. This recognition is carried out so casually that in many cases we are not aware of the differences between objects that seem alike to us. Shape recognition has many applications in content based image retrieval [1],[2], categorizing objects [3],[4], biological image processing [5], optical character recognition [6], and so forth [7]. The fundamental characteristic of shape recognition is categorizing objects based on their geometry. However, a shape category may contain hundreds of slightly different instances. These dissimilarities are modeled by different means. A common approach is using graphs of nodes interconnected by strings [8]. These approaches assume that the model topology is an important shape feature [9]. The total energy of the system is minimized through a cost function and the shape is the graph of nodes and springs in its equilibrium. A modified form of spring graph model is representing the deformation through a transform. Here the assumption is that the corresponding nodes of the graph can be mapped to the nodes of the generic model through an affine or a non-linear transform [10], [11]. In practice however, the dissimilarities between the shapes of a category cannot be represented by a single transform. Besides, external factors such as photometric variation can greatly affect the detection of salient points in a shape and hence matching process. In [12] the authors propose a method for partial matching of 3D objects. Their approach uses the size of a part relative to the whole object, and the number of curvature changes and strength as the salient features for partial matching. They associate a number of rotation-and-scale invariant indices with each salient feature to accelerate matching operations. Probabilistic models are also utilized to extract the most and the least probable deformation in a generic representative of a shape [13], [14]. These models require a large dataset encompassing all variations which is difficult to acquire in many cases. Besides, representing articulated and deformable shapes is subject to error. To deform the model, affine [15], [16] similarity [17], [18] and polynomial [19] transformations have been used. At each iteration, the similarity between the model and the input image is re-computed. These models which are referred to as Atlas suffer from the complexity of the morphing step. They also require a large manually segmented and annotated data set for developing the initial model [20], [16], [19], [21]. The first step in model-based segmentation which tries to roughly align the model to the input image comprises of a 3-dimensional registration and a 2-dimensional rotation/scaling/translation steps if the model is a 3-dimensional volumetric model. The registration and alignment steps in this process require salient points having the properties of being detectable in both input image and model, being invariant with respect to the patient, disease, and applied treatment, and being capable of determining the image position in the 3-dimensional model.

Shape descriptors are also defined based on the histograms [22], [23] however, these descriptors are not scale-invariant. Shape context is one of the methods utilized for the general problem of shape matching when the shapes differences are not limited to those coming from affine transforms [24], [25], [26], [27]. In fact, shape matching covers the extensive research work carried out to measure the distance between shapes in terms of similarity. Two category of similarity methods have been considered for comparing shapes which are methods based on the features extracted from a shape, and methods based on the appearance of the shape. Feature based methods have been used with features such as silhouette, object boundaries, corner points, Fourier descriptors, etc. Spatial distribution of the feature points have also been considered for shape matching. For instance, the method given in [28] uses feature point locations for voting for a model. The main advantage of the method is avoiding an explicit matching of the feature points. A comparative study of the feature based methods for shape matching has been given in [25]. The appearance based methods try to find the correspondence

Digital Object Identifier 10.4316/AECE.2015.01019

between pixels using similarity of their gray level values [29]. Grouping the pixels into models such as deformable templates is among the attempts to make the method insensitive to certain transforms [30], [31]. The main disadvantage of these models is the need for human intervention in designing the model. The second group of approaches considers learning the statistical features of the gray-level pixels. Principal component analysis (PCA) is the most commonly used method from this group which is the basis for many face detection and identification solutions [32].

Shape context considers a subset of the pixels of an object as its descriptors. The spatial distribution of these pixels is used as the similarity metric for comparing the objects. Therefore, shape context has characteristics from both groups of shape matching algorithms. Shape contexts have the property of grouping feature points according to their spatial distributions and relaxing the one-to-one correspondence requirement for shape matching. In [33] quad-trees are used for adaptive resolution representation of shapes after rotation and scaling. Their method of representing a shape is designed for solid single component objects and is not capable of matching articulated objects, or objects with multiple disjoint components. Beside to shape context, shape axis trees are also used for matching shapes. In representing shapes using a shape axis tree, the main axis of the shape is extracted and utilized.

Figure 1 depicts sample shape and the corresponding shape axis.

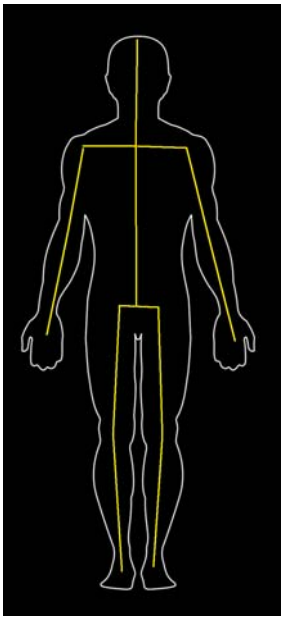

Figure 1: Sample shape and its shape axis

In [34] a compact and stable shape representation named shape axis is presented. They use the self-similarity of the shape to define the shape axis. In their method a set of corresponding boundary points are determined. Connecting the corresponding points, line segments are found. Finally these line segments are used for defining the shape axis by connecting their mid points. Special tree data structures are used for representing shape axis. The shape axis tree stores ending points of the shape axis in is leaf nodes while, junctions are stored as internal nodes. Although the main structure of the shape is captures by the shape axis representation, in articulated objects, matching can pose challenges.

Transform domain shape representation is also used for shape matching. Fourier descriptors are used by authors in [35] and [36] to represent the boundary features. In [37] authors report a method to represent the internal area of a shape using Radon transform. As the Radon transform of an image is defined by the set of projections along lines taken at different angles, they define their descriptors as a matrix of frequencies computed on the Radon transform of an image aggregated by the angle parameter of the Radon transform. The main issues in their method have been the sensitivity of the method to noise and the difficulty of determining the descriptor size.

In [38] the authors use the idea that the appearance of an interest region can be well characterized by the distribution of its local features. They use Scale-invariant feature transform (SIFT) descriptor to find and use gradient as the local feature. Besides, they introduce a texture feature called center-symmetric local binary pattern (CS-LBP) which is a modified version of the local binary pattern feature. They combine the SIFT and CS-LBP as their shape feature.

3D shape perception and retrieval have been discussed in many shape matching applications. The main application of these methods is matching building models. Therefore, the databases used in these systems have been restricted to geometrical shapes. Some of these shapes have been illustrated in Figure 2.

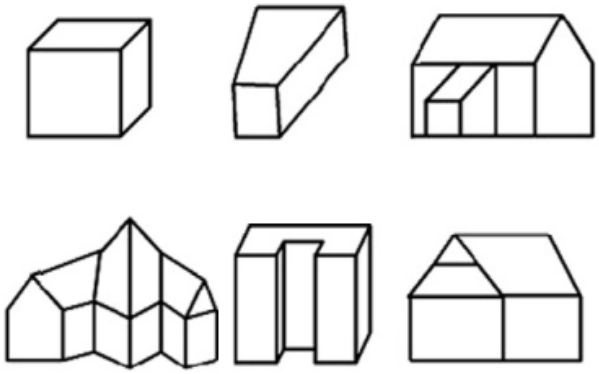

Figure 2: Different types of 3D building models

Many proposed method however, convert the 3D models into a multiple of 2D shapes characterizing the 3D shape from different viewpoints. Silhouettes for instance have been utilized by the author in [39] to describe a 3D volume. The authors in [40] report on using sketches as input to their retrieval system. In [41] authors introduce a method based on 3D features extracted from shapes. Their method consists of three main steps:

1. Normalization: This step performs translation, scaling and horizontal rotation.
2. Feature extraction: They use two features namely shell and unevenness. Shell is defined as the bounding box of the shape, while unevenness includes features such as circularity, eccentricity, and Fourier descriptors.
3. Matching: They define a feature vector for each shape and consider the angle between the vectors to decide whether the shapes match or not.

The main challenge in 3D shape modeling is related to the complexity arising from complex and multiple shapes, many researchers have only considered the case of single and

isolated shapes having geometric models.

Ma and Latecki [42] proposed a shape matching method which is based on defining a shape context for boundary segments and using an object localization algorithm as maximal clique computation in a weighted graph for partial object detection. Since their method is similar to our proposed method in terms of matching shape components in the first stage, and considering the relative position of the detected components for shape matching, we compare the experimental results of our method with their results. Assuming that a boundary segment is given by a planar set X, the shape context proposed in [42] is defined as both the length and direction of the vectors from xϵX to all other points in X. In order to compare boundary segments, they define a distance matrix named A_D and an angle difference matrix named A_Θ. These matrices are defined in Equation 1.

$$A_D(P,Q,T,U)=\exp\left(-\frac{(D^{(P,Q)}(i,j)-D^{(T,U)}(i,j))^2}{(D^{(P,Q)}(i,j)\delta)^2}\right)$$
$$A_\Theta(P,Q,T,U)=\exp\left(-\frac{(\Theta^{(P,Q)}(i,j)-\Theta^{(T,U)}(i,j))^2}{\delta^2}\right) \quad (1)$$

where P,Q,T, and U are point sets representing four boundary segments, $D^{(X,Y)}(i,j)$ is the distance from boundary segment X to boundary segment Y, and $\Theta^{(x,y)}(i,j)$ is defined as the orientation of vectors x_i - y_j. They define their similarity criteria as:

$A(P, Q, T, U) = A_D(P, Q, T, U) + A_\Theta(P, Q, T, U)$

which measures the similarity between two shapes assuming boundary segments *P* and *Q* are from the first shape, and boundary segments *T* and *U* are from the second segment. Assuming each boundary segment as a node of a graph, the authors use a maximal clique computation in a weighted graph for shape matching.

The method proposed in [34] uses a two-stage shape matching and hence similar to our proposed method. We have considered this method one of the benchmarks for verifying the performance of our method. Our main contribution is introducing a method for representing objects of multiple (probably disjoint) components, and the necessary algorithms for measuring their similarities and matching them.

In the following section we introduce our multi-level shape representation model and the feature vector used for registration of the image with the model. Then we introduce our experimental set-up and evaluation metrics. The results and their analysis conclusions are presented subsequently.

II. Proposed Method

The proposed method is based on a multi-level shape representation. In the following sections, representing components at each layer and their matching algorithms are presented.

Representing Components

The lowest level in this model uses a scale and orientation invariant approach to represent each component. However, the size and orientation parameters are computed and used in the upper level for multi-component shape matching. Besides, minor boundary deformations are smoothed out to avoid over-fitting of the comparison algorithm to the generic shape model of the component.

Our assumption is that the shape is provided as a binary area. This assumption is compatible with the results obtained from the threshold filtering algorithms. In order to make the shape orientation invariant, the coordinates of the shape boundary in a bounding box have been utilized. Assuming the lower left corner of the bounding box as the origin of the coordinate system, each shape boundary pixel is considered as a vector such as $x=(a,b)^T$ where *a* and *b* are the coordinates of the boundary pixels.

We then compute the covariance matrix for the boundary pixel vectors. The shape is rotated to align the coordinate axes with the eigenvectors of the covariance matrix of boundary pixels. The amount of rotation is preserved as the *orientation* feature of the component for comparison stage. A new bounding box parallel to the new coordinate system is defined for the shape. The width and height of the bounding box are normalized with respect to the length of the multi-component shape and stored as *normalized size* feature of the component.

Figure 1 depicts a vertebrae segmented from a CT image and rotated to align with the eigenvectors of the covariance matrix of its boundary pixels.

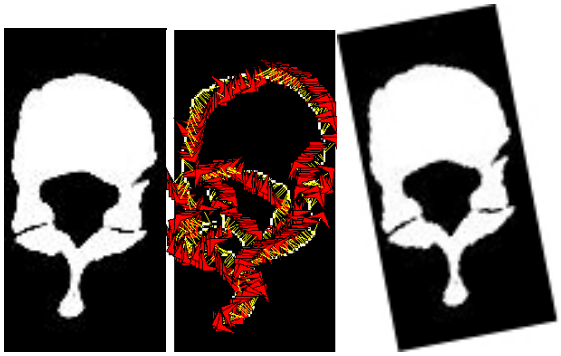

Figure 3. Segmented area of vertebrae from a CT image (left), Direction of edge pixels (middle), Vertebrae after being aligned with the eigenvectors of the covariance matrix of its boundary pixels (right).

To represent the shape, we consider utilizing a quad tree to describe the shape area. To handle the minor difference along the boundary of the shape, we restricted the minimum size of any side of the rectangular cells in the quad tree to 4. Besides, the cells are not split if at least 90% of the pixels have the same intensity value. This relaxing measurement helps us avoid creating trees with large heights. Besides, minor changes are ignored in the initial stage of estimating the shape. However, for each cell, size, intensity, and purity parameters are defined. *Intensity* parameter specifies whether the cell is part of the shape or the background and is the intensity value of the majority pixels falling in that cell, while *purity* defines the ratio of the pixels having cell intensity value (*Intensity* parameter) to the total number of pixels falling into that cell. Hence if 75 out of 100 pixels in a cell are black the *Intensity* will be black and the *purity* will be 0.75.

Figure 4 depicts the quad tree created using the bounding box of the shape shown in Figure 3.

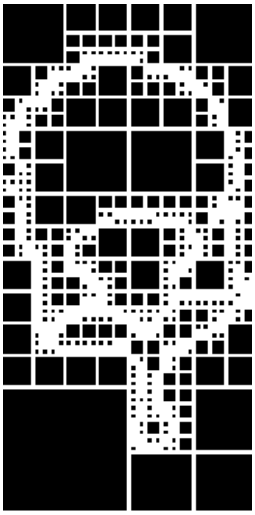

Figure 4. Quad tree representation of the segmented area of vertebrae from a CT image

Shape Matching

In this section we present our proposed algorithm for matching shapes of single components. Later on we present our method for representing the multi-component shapes, and matching them. Assuming that the shapes to be matched have been rotated and aligned with the eigenvectors of their covariance matrices, a minimum bounding box is used to define their extension, and are represented using the modified quad-tree. We match the shapes as shown in Algorithm 1.

Algorithm 1. Matching shapes represented by quad-trees

→Similarity (input: QTree1, QTree2; Output: SimilarityValue)
→IF QTree1.Root.Purity > 0.9 AND QTree2.Root.Purity >0.9 THEN
» IF QTree1.Root.Intensity = QTree2.Root.Intensity THEN
▪ SimilarityValue = Min (QTree1.Root.Purity, QTree2.Root.Purity)
» ELSE
▪ SimilarityValue = 1-Max (QTree1.Root.Purity, Qtree2.Root.Purity)
→ELSE IF QTree1.Root.Purity > 0.9 THEN
» SimilarityValue = QTree2.Root.Purity
→ELSE IF QTree2.Root.Purity > 0.9 THEN
» SimilarityValue = QTree1.Root.Purity
→ELSE
» SimilarityValue =

$$\frac{1}{4}\sum_{i=1}^{4} Similarity(QTree(1).Root.Child(i), QTree(2).Root.Child(i))$$

Since the leaf nodes of the quad tree either have a purity value of 0.9 or contain no more than 16 pixels, the proposed algorithm finds the sum of minimum purity values of corresponding cells in both shapes. The algorithm assumes the components have been oriented along their covariance matrix eigenvectors. However, there exists the possibility of a 180-degree rotation difference between the two components. To consider these cases, the quad tree of the component after 180-degree rotation is also compared with the reference quad tree.

Multi-Component Shape Representation

The proposed multi-layer model defines a spatial tree to represent the components of the shape in the second layer. The tree is constructed based on a root or origin which is located at the centroid of the shape. Each component is represented by its spatial features, and shape features. Spatial features of a component are the angles of the arc of the circular sector in a counter clockwise measurement encompassing the component, and the distance from the centroid of the component to the root of the tree. Figure 5 depicts the spatial features of a sample component.

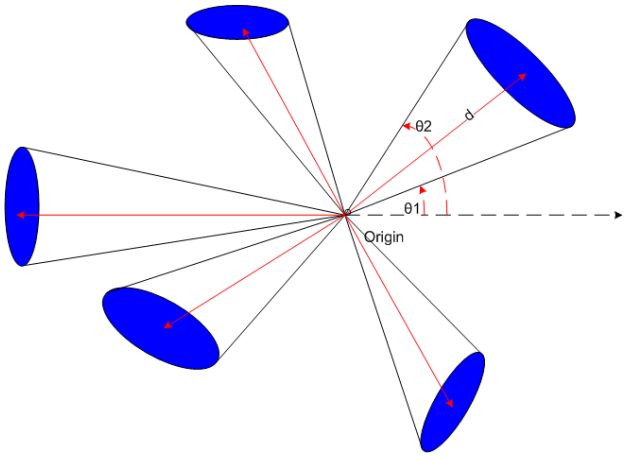

Figure 5. Spatial features of each shape component: the angles describing the circular sector encompassing the component (θ1 and θ2), and the distance of the centroid of each component to the shape origin (d).

Shape features are the feature values obtained from level one of the multi-layer model (quad-tree representation, orientation, and normalized size). To represent a component using its spatial features, we have used a K-d tree data structure. The first level in our K-d tree represents the angles of the arc of a circular sector containing at least one component. If a circular sector contains more than one component, level two distinguishes them by considering the distance of their centroids to the origin of the tree. Figure 6 depicts a sample shape and Figure 7 its K-d tree representation.

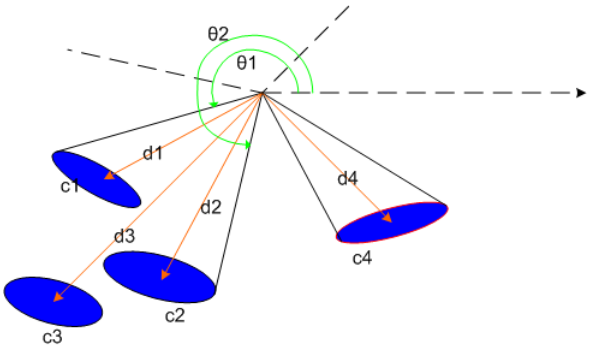

Figure 6. A sample multi-component shape

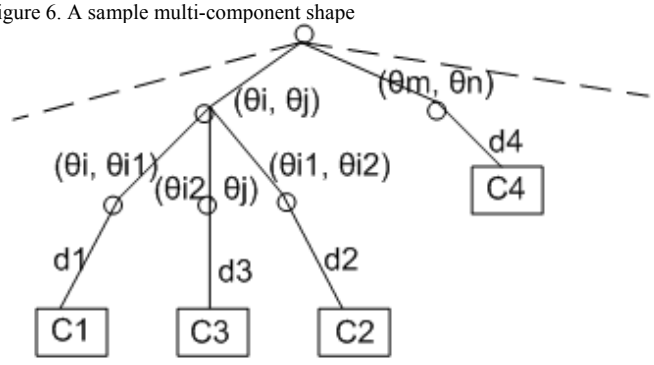

Figure 7. The K-d tree representation of the multi-component shape shown in Figure 6.

It should be noted that the branches of the K-d tree at the second level are sorted according to their distance to the shape origin. At the leaves of the K-d tree we store the

components. Each component is represented by its normalized size, orientation and shape features of its quad-tree.

Multi-Component Shape Matching

The final step in our proposed method is matching the K-d spatial trees representing the multi-component shapes. The intuitive description of our comparison method is as below:

Two shapes are similar iff

» They contain the same number of components,
» The spatial features of the components namely, relative location with respect to the shape origin, orientation, and normalized sizes are the same,
» The corresponding components have the same shape.

The first two similarity criteria are verified by comparing the K-d trees of the shapes. The comparison is based on computing a cost function which objectively measures the difference between the two K-d trees. The cost function of our method is a weighted sum of the similarity values obtained from tree structure comparison, and component similarities. Equation 2 defines the spatial similarity metric between components where $W_{1,2,3}$ are the weight values of the equation.

$$\begin{aligned}\text{Component}_{\text{spatial similarity}} = {} & W_1 \times |\text{C1.distance} - \text{C2.distance}| + \\ & W_2 \times |\text{C1.Arc}_{\text{begin}} - \text{C2.Arc}_{\text{begin}}| + \\ & W_3 \times |\text{C1.Arc}_{\text{end}} - \text{C2.Arc}_{\text{end}}|\end{aligned} \quad (2)$$

We find the corresponding component of each component by comparing each component from the first shape with all components of the second shape, and each component of the second shape with all components of the first shape (cross correlation). The lowest component spatial similarity values give the correspondences. The shape similarity cost value is defined as a weighted sum of total component spatial similarity values and component shape similarity as shown in Equation 3.

$$\begin{aligned}Cost = {} & \frac{W_1}{c}\sum_{i=1}^{c} Component_{spatial\_similarity}(i) + \\ & \frac{W_2}{c}\sum_{i=1}^{c} Similarity(i) + \\ & \frac{W_3}{c}\sum_{i=1}^{c} OrientationDiff(i) + \\ & \frac{W_4}{c}\sum_{i=1}^{c} SizeDiff(i)\end{aligned} \quad (3)$$

Cost function considers the corresponding components for finding the differences. The second term (Similarity) is computed as given by Algorithm 1. OrientationDiff is the difference in orientation of the corresponding components. Finally SizeDiff defines the size feature difference between the corresponding components. Weight values have been empirically set in our experiments as W_1=0.2, W_2=0.35, W_3=0.15, and W_4=0.3. Here the tree structure similarity value is normalized with the number of components (parameter C). This means that as the number of components grows larger, the impact of a missing component on the similarity metric becomes smaller. Besides, the total similarity value of the components is normalized using the number of components to reduce the effect of single component dissimilarity when the shape contains a large number of components.

The proposed method has the following properties:

- The boundary information is combined with the area occupied by each component during the first stage of the shape matching. This is in contrast to the other shape matching methods where only the shape and orientation of the boundary segments are considered as the similarity metric.
- If an object is composed of two or more disjoint segments (or the current imaging conditions results in such a view of the object), the relative size, orientation, and location of each component become of importance during the matching stage. The proposed method considers all these features during the second stage of the shape matching procedure.
- The proposed method is scale and rotation invariant. Besides, minor variations of the boundary do not affect the matching process.

The main disadvantage of the proposed method is its sensitivity to partial occlusion. Incomplete data can result in the different number of detected components which will cause a mismatch. We are considering the case of shape matching using incomplete data as our future work.

III. Experimental Results and Analysis

The experimental verification of the proposed method was carried out using two sets of images. The first set contains nine object categories with no articulation from McGill 3D shape benchmark database where we have used their 2D images (Figure 8). The second set consists of ten series of abdominal CT images. The CT images are obtained from helical CT scanners, with slice thickness of 1.25mm, and dimension of 512 × 512 pixels. For this experiment, a model of the human chest was created by applying threshold to CT images and extracting thoracic skeleton. Manual cleaning of the threshold filtered images was necessary to remove some areas corresponding to the examination bed. The model was created by averaging 10 different abdominal CT image series. The model therefore, includes values ranging from zero (no bone) to 10 (bone seen in all 10 series).

Four CT examination series are used for testing the algorithm. Single images from different positions of the test series were used for evaluation. Choosing images from the test series is carried out randomly however, we restricted the range to the area covered by liver.

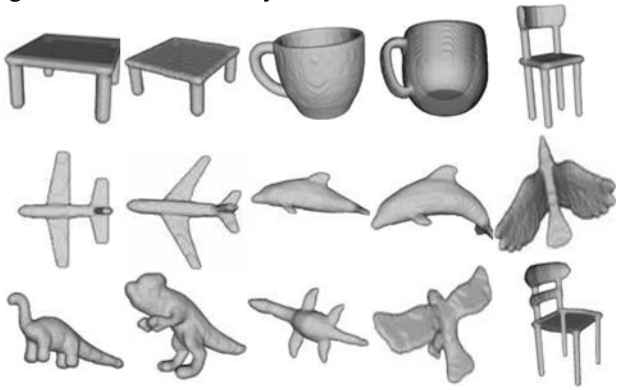

Figure 8. Sample images from McGill non-articulated objects categories.

Figure 9 depicts a threshold filtered sample image from

our test series (left), and the most similar slice in the first series (right).

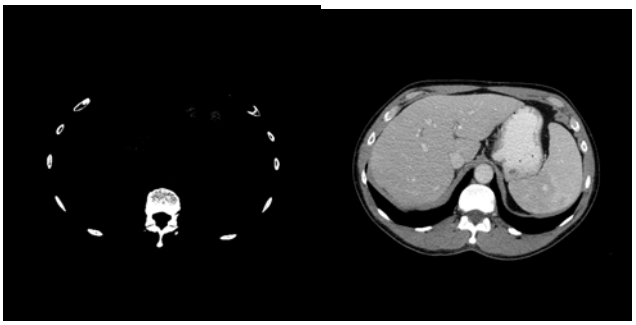

Figure 9. Threshold filtered sample input image (left), and the result of matching it with an abdominal CT examination series (right).

Two types of experiments are conducted to verify the performance of the proposed method. The first set of experiments, consider the matching of local areas or components. Hence, it measures the performance of our quad-tree based shape context algorithm. The images from McGill non-articulated objects categories are utilized in these experiments. In this experiment, each image from a category is considered and matched with all images in one category (Figure 10), and multiple categories (Figure 11). The second set is designed to evaluate the multi-component matching algorithm. For the second experiments we are using abdominal computed tomography images where each threshold filtered cross-section of a bone (ribs) is considered as a component and the threshold filtered image of the thoracic skeleton comprises the multi-component object to be matched (figure 9. left).

Figures 10 and 11 depict the result of applying our proposed method to match single component objects which is the first stage of our algorithm.

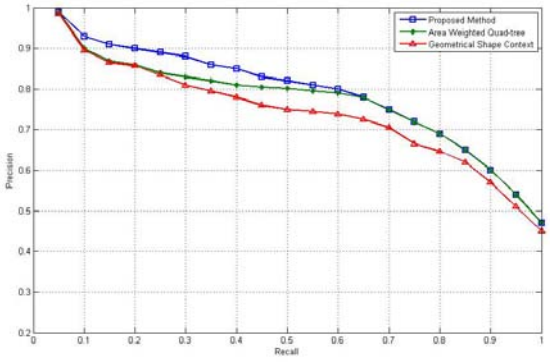

Figure 10. Precision-recall (PR) plot for three shape descriptors, applied to single categories of the McGill database of non-articulated shapes.

Our quad-tree geometry representation method assumes the cells of the quad-tree have the same importance, and the purity of a cell is the determining factor. As a benchmark we have modified the proposed matching criteria to include the area of the cell as given below:

SimilarityValue =
Min (QTree1.Root.Purity, QTree2.Root.Purity)×QTree1.Root.Area

Since the tree is defined recursively, the root area returns the area of the quadrant pointed to y that tree branch. Meanwhile, the shape context based matching method proposed in [25] has been considered as a second benchmark in comparing the results of our proposed method.

The outputs of the experiments indicate that the proposed method outperforms both other methods. The reason for this better performance is two-fold. Firstly, since the matching of the components is scale invariant and the size is passed as a parameter to the next stage, the main deterministic factor becomes the shape of the contour surrounding the component and hence, the internal area should not be considered with a large weight factor. Secondly, statistical distribution of the boundary pixels cannot be a reliable factor in comparing shapes if the shapes are close in geometry. This means the shape context as proposed in [25] fails if the number of bins is small.

The second group of experiments compares the multi-component shapes using the results of the first stage of matching process. For these experiments we use abdominal CT images where a threshold is applied to the image to extract the bones of the thoracic skeleton. Each bone cross-section is considered as a component. The input images are compared with a set of threshold filtered abdominal CT images which are considered as a 3D reference model. In these experiments, we have considered the method described in [25].

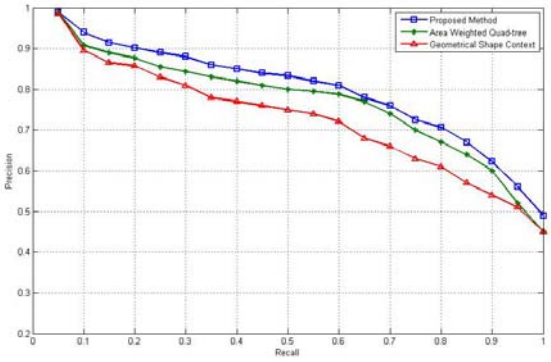

Figure 11. Precision-recall (PR) plot for three shape descriptors, applied to multi-categories of the McGill database of non-articulated shapes.

The better performance of our proposed method is an indicator of the importance of applying shape matching in two levels: a local matching which is carried out in terms of components, and a global matching which benefits from the results of the first level.

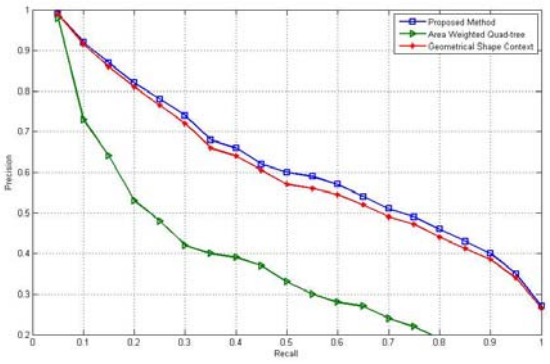

Figure 12. Precision-recall (PR) plot for three shape descriptors, applied to multi-component images of abdominal CT images.

The poor performance of area weighted quad-tree method

indicates that the quad-trees are suitable for representing single component objects as is shown in Figures 10 and 11, however, multi-component shapes are not represented effectively because any change in the position, orientation, or size of a component affects the whole model drastically.

The method has been modified to contain a shape context of radial parts which are 10 degrees apart, and include 5 layers. This implementation is used as a benchmark where its results are compared with the results of the proposed method as shown in Figure 12.

Our third set of experiments compares the performance of the proposed method with the method proposed in [42]. We used three sets of shapes including simple, articulated, and threshold filtered medical images. In simple and articulated images, the rates are found by counting the number of times the test image is classified correctly. In case of medical images, we have counted the number of times that the best match for a sample image is found in a series of CT examination from abdomen. The results of applying the algorithms are given in Table 1.

Table 1. Comparative detection rates using different categories of images

	Simple Shapes	Articulated Shapes	Medical Images
Method proposed by Latecki [34]	89%	80%	64%
Proposed method	94%	88%	83%

The method proposed in [42] considers boundary segments normalized separately before comparison. This results in matching images of the same object with affine shape differences. Besides, in shapes with multiple disjoint components such as threshold filtered medical images, the orientation metric proposed in [42] shows a poor performance. This is indicated in Table 1 where the performance of the method is quite high in simple object images but very poor in medical images. The second stage of our proposed method clearly outperforms their proposed method.

IV. Discussion

A two-layer shape context based method has been proposed for matching multi-component objects. The proposed method matches the components using the shape geometry which is represented by a quad-tree. The representation is rotation and scale invariant, and minor differences in the object boundary do not affect the matching process. However, the size and orientation of the component are utilized in the next stage where the multi-component matching is carried out. The experimental results illustrate that the method is very versatile in matching objects which are made of disjoint components. An important application for the proposed method is medical and biological images. In our experiments, we used CT images of abdomen where the bones had been threshold filtered in matching with a statistical 3D model. However, biological images such as microscopy images of Electron Microscopy Tomography (EMT) are a good application area for our proposed method. In our proposed method the geometric features are of equal importance however, the performance of the method can also be improved by assigning different weights to the features. For instance xiphoid process of sternum is an indicator of the topmost location of liver in transversal abdominal CT images and can be considered with a higher weight.

References

[1] P. Daras, S. Manolopoulou, and A. Axenopoulos, "Search and Retrieval of Rich Media Objects Supporting Multiple Multimodal Queries", IEEE Transaction on Multimedia, vol. 14, no. 3, June 2012, DOI: 10.1109/TMM.2011.2181343

[2] M. Worring and T. Gevers, "Interactive retrieval of color images", International Journal of Image Graphics, vol. 1, no. 3, pp. 387-414, 2001, DOI: 10.1142/S0219467801000244

[3] S.B. Kang and K. Ikeuchi, "The Complex EGI: A New Representation for 3D Pose Determination", IEEE Transaction on Pattern Analysis and Machine Intelligence, vol. 15, no. 7, pp. 707-721, 1993, DOI: 10.1109/34.221171

[4] T. Zaharia and F. Prteux, "Shape-Based Retrieval of 3D Mesh Models", Proceedings of IEEE International Conference on Multimedia and Expo, 2002, DOI: 10.1109/ICME.2002.1035812

[5] J. S. Nalewajko, S. Jezewski, R. Ambroziak, and M. Kuzariski, "Digital image processing methods in biological structure recognition - a short review", Proceedings of the 2nd International Conference on Perspective Technologies and Methods in MEMS Design, pp. 61-64, 2006, DOI: 10.1109/MEMSTECH.2006.288664

[6] C. C. Tappert, C. Y. Suen, and T. Wakahara, "The state of the art in online handwriting recognition", IEEE Transactions on Pattern Analysis and Machine Intelligence, vol. 12, no. 8, pp. 787-808, 1990, DOI: 10.1109/34.57669

[7] Y. Mingqiang, K. Kidiyo, and R. Joseph, "A survey of shape feature extraction techniques", Pattern Recognition Techniques, Technology and Applications, ISBN: 978-953-7619-24-4, pp. 43-90, 2008, DOI: 10.5772/6237

[8] M. A. Fischler, and R.A. Elschlager, "The Representation and Matching of Pictorial Structures", IEEE Transactions on Computers, vol. C-22, no.1, pp. 67-92, 1973, DOI: 10.1109/T-C.1973.223602

[9] H. Sundar, D. Silver, N. Gagvani, and S. Dickson, "Skeleton based shape matching and retrieval", In Proceedings of Shape modeling International, Seoul, Korea, pp. 130-139. 2003, DOI: 10.1109/SMI.2003.1199609

[10] D. Zarpalas, P. Daras, A. Axenopoulos, D. Tzovaras, and M. G. Strintzis, "3D model search and retrieval using the spherical trace transform", EURASIP Journal of Advanced Signal Processing, vol. 2007 no. 1, pp. 1-15, 2007, DOI:10.1155/2007/23912

[11] S. Loncaric, "A survey of shape analysis techniques", Pattern Recognition, vol. 31, no. 8, pp. 983-1001, 1998, DOI:10.1016/S0031-2023(97)00122-2

[12] R. Gal, and D. Cohen-Or, "Salient geometric features for partial shape matching and similarity", ACM Transaction on Graphics, vol. 25, no. 1, pp. 130–150, 2006, DOI: 10.1145/1122501.1122507

[13] A. Joly, O. Buisson, and C. Frelicot, "Content-based copy retrieval using distortion-based probabilistic similarity search", IEEE Transaction on Multimedia, vol. 9, no. 2, pp. 293-306, 2007, DOI: 10.1109/TMM.2006.886278

[14] C. B. Akgul, B. Sankur, Y. Yemez, and F. Schmitt, "3D Model Retrieval Using Probability Density-Based Shape Descriptors", IEEE Transaction on Pattern Analysis and Machine Intelligence, vol. 31, no. 6, pp. 1117-1133, 2009, DOI: 10.1109/TPAMI.2009.25

[15] M. B. Cuadra, C. Pollo,A. Bardera, O. Cuisenaire, J. G. Villemure, and J. P. Thiran, "Atlas-Based Segmentation of Pathological MR Brain Images using a Model of Lesion Growth", IEEE Transaction on Medical Imaging, vol. 10, no. 23, pp. 1301–1314, 2004, DOI: 10.1109/TMI.2004.834618

[16] Q. Dai and K. J. Singleton, "Specification analysis of affine term structure models", Journal of Finance, vol. 55, pp. 1943–1978, 2000, DOI: 10.1111/0022-1082.00278

[17] S. A. Shimizu, R. Ohno, T. Ikegami, H. Kobatake, S. Nawano, and D. Smutek, "Multi-organ Segmentation in Three Dimensional Abdominal CT Images", International Journal of Computer Assisted Radiology and Surgery (CARS), vol. 1, no. 7, pp. 76–78, 2006.

[18] D. J. Montagnat, "Volumetric Medical Images Segmentation using Shape Constrained Deformable Models", CVRMed-MRCAS, Lecture notes in Computer Science, vol. 1205, pp. 13–22, 1996, DOI: 10.1007/BFb0029220

[19] D. Y. Nakayama, Q. Li, S. Katsuragawa, R. Ikeda, Y. Hiai, K. Awai, S. Kusunoki, Y. Yamashita, H. Okajima, Y. Inomata, K. Doi, "Automated Hepatic Volumetry for Living Related Liver Transplantation At Multisection CT", Radiology, vol. 240, no. 3, pp. 743-748, 2006, DOI: 10.1148/radiol.2403050850

[20] H. S-J. Lim, Y.-Y. Jeong, and Y.-S. Ho, "Automatic liver segmentation for volume measurement in CT Images", Journal of Visual Communication and Image Representation, vol. 17, no. 4, pp. 860–875, 2006, DOI:10.1016/j.jvcir.2005.07.001

[21] K. J. Lee et.al, "Efficient liver segmentation using a level-set method with optimal detection of the initial liver boundary from level-set speed images", Computer Methods and Programs in Biomedicine, vol. 88, no. 1, pp. 26-38, 2007, DOI:10.1016/j.cmpb.2007.07.005

[22] D. Huber. and M. Herbert, "Fully automatic registration of multiple 3d data sets", Image and Vision Computing, vol. 21, no. 7, pp. 637-650, 2003, DOI: 10.1016/S0262-8856(03)00060-X

[23] A. Frome, D. Huber, R. Kolluri, T. Bulow, and I. Malik, "Recognizing objects in range data using regional point descriptors", In Proceedings of the European Conference on Computer Vision (ECCV), 2004, DOI: 10.1.1.2.7940

[24] V. Monga and B.L. Evans, "Perceptual image hashing via feature points: performance evaluation and tradeoffs", IEEE Transactions on Image Processing, vol. 15, no. 11, pp. 3452–3465,2006, DOI: 10.1109/TIP.2006.881948

[25] S. Belongie, J. Malik, and J. Puzicha, "Shape matching and object recognition using shape contexts", IEEE Transactions on Pattern Analysis and Machine Intelligence, pp. 509–522, 2002, DOI: 10.1109/34.993558

[26] L. Xudong and Z. J. Wang, "Shape Context based Image Hashing using Local Feature Points", 18th IEEE International Conference on Image Processing (ICIP), pp. 2541 - 2544 , 2011, DOI: 10.1109/ICIP.2011.6116181

[27] B. Moghaddam, T. Jebara, and A. Pentland, "Bayesian Face Recognition", Pattern Recognition, vol. 33, no. 11, pp. 1771-1782, 2000, DOI:10.1016/S0031-3203(99)00179-X

[28] X. Zhang, and Y. Liu, "Point Pattern Matching for Articulated or Multiple Objects", Proceedings of the 17th International Conference on Pattern Recognition (ICPR'04), vol.3, pp. 630 – 633, 2004, DOI: 10.1109/ICPR.2004.1334608

[29] D.G. Lowe, "Distinctive image features from scale-invariant keypoints," International journal of computer vision, vol. 60, no. 2, pp. 91–110, 2004.

[30] H. Chui, and A. Rangarajan, "A New Algorithm for Non-Rigid Point Matching", Computer Vision and Pattern Recognition, vol. 2, pp. 44 – 51, 2000, DOI: 10.1109/CVPR.2000.854733

[31] L.J. Latecki, R. Lakamper, andT. Eckhardt, "Shape Descriptors for Non-Rigid Shapes with a Single Closed Contour", IEEE Conference on Computer Vision and Pattern Recognition, vol.1, pp. 424–429, 2000, DOI: 10.1109/CVPR.2000.855850

[32] M. Sharkas,and M.A.Elenien, "Eigenfaces vs. fisherfaces vs. ICA for face recognition; a comparative study", 9th International Conference on Signal Processing (ICSP 2008), pp 914-919, 2008, DOI: 10.1109/ICOSP.2008.4697276

[33] K. Chakrabarti, M. O. Binderberger, K. Porkaew, and S. Mehrotra, "Similar shape retrieval in MARS", IEEE International Conference on Multimedia and Expo (ICME), vol. 2, pp. 709-712, 2000, DOI: 10.1109/ICME.2000.871460

[34] T. L. Liu, D. Geiger, and R. V. Kohn. "Representation and self-similarity of shapes", International Conference on Computer Vision (ICCV), pp. 1129–1135, 1998, DOI: 10.1109/TPAMI.2003.1159948

[35] Y. Rui, A. She, T. S. Huang, "A Modified Fourier Descriptor for Shape Matching in MARS", Image Databases and Multimedia Search, pp. 165–180, 1998, DOI: 10.1.1.42.5799

[36] D. Zhang and G. Lu, "Review of shape representation and description techniques", Pattern Recognition, vol. 37, pp. 1-19, 2004, DOI: 10.1016/j.patcog.2003.07.008

[37] S. Tabbone and O. Ramos Terrades and S. Barrat, "Histogram of Radon Transform. A useful descriptor for shape retrieval", 19th International Conference on Pattern Recognition (ICPR), pp. 1-4, 2008, DOI:10.1109/ICPR.2008.4761555

[38] M. Heikkila, M. Pietikainen, C. Schmid, "Description of interest regions with local binary patterns", Pattern Recognition, vol. 42, no. 3, pp.425-436 2009, DOI:10.1016/j.patcog.2008.08.014

[39] D. Chen, X. Tian, Y. Shen, O. Ming, "On visual similarity based 3D model retrieval", Computer Graphics Forum, vol. 22, no.3, pp. 223–232, 2003, DOI: 10.1111/1467-8659.00669

[40] T. Funkhouser, P. Min, M. Kazhdan, J. Chen, A. Halderman, D. Dobkin, D. Jacobs, "A search engine for 3D models". ACM Transaction on Graphics, vol. 22, no.1, pp. 83-105, 2003, DOI: 10.1145/588272.588279

[41] M. Zhang, L. Zhang, T. Mathiopoulos, Y. Ding, H. Wang, "Perception-based shape retrieval for 3D building models", ISPRS Journal of Photogrammetry and Remote Sensing, vol. 75, pp. 76–91, 2013, DOI:10.1016/j.isprsjprs.2012.10.001

[42] T. Ma and L. J. Latecki, "From Partial Shape Matching through Local Deformation to Robust Global Shape Similarity for Object Detection", IEEE Conference on Computer Vision and Pattern Recognition (CVPR), pp. 1441–1448, 2011, DOI: 10.1109/CVPR.2011.5995591